CO_2 Transfer Across a Liquid Membrane Facilitated by Carbonic Anhydrase

Lihong Bao[1], Stefanie L. Goldman[1] and Michael C. Trachtenberg[2]

[1]Carbozyme Inc., 1 Deer Park Dr., Ste. H-3, Monmouth Jct., NJ 08852
[2]Sapient's Institute, 1 Deer Park Dr., Ste. H-3, Monmouth Jct., NJ 08852

Introduction

Increasing atmospheric levels of CO_2, in large part due to anthropogenic combustion of energy yielding hydrocarbons, portends significant if not catastrophic weather related events. One strategy to stabilize atmospheric CO_2 levels is to capture the post-combustion product for disposal or, preferably, commercial use. The latter case, in particular, requires the development of both effective and economic methods. The requirements are stringent. Currently available methods, such as conventional amine absorption/stripping do not suffice because of their heavy energy requirement. Better means for post-combustion separation and capture of CO_2 are being investigated extensively [1,2,3,4,5].

Microporous hollow fiber membrane modules offer several advantages over a conventional packed absorption towers. The most obvious ones are very high specific area for gas-liquid contact, independent phase flow, and easy scale-up. These benefits make membrane designs strong candidates for CO_2 separation applications [6]. Commonly, microporous hollow fiber membrane modules function as gas/liquid contactors [1,2,3]. Another common usage of microporous hollow fiber membrane is in supported liquid membrane (SLM) designs, in which a liquid phase is immobilized in the pores of a microporous membrane interposed between two other phases (liquid or gas). High separation factors can be achieved through facilitated transport in the liquid phase in the pores [7]. However, SLMs have not been adopted for large-scale gas separation because of their lack of long-term stability.

We are developing a novel, enzyme-catalyzed, contained liquid membrane (CLM), hollow fiber reactor to separate CO_2 from a wide variety of primary sources including flue gas and natural gas [8,9]. In the CLM reactor, two sets of identical microporous hollow fibers are used such that the feed gas flows through the lumen of one set of fibers while the sweep gas/liquid passes through the lumen of the other set. A liquid phase is contained in the space outside of the hollow fibers (shell side). This liquid can be circulated through external means as may be warranted. Thus the reactor is stable through continual replenish of fresh liquid. In addition, the liquid membrane operation is facilitated by use of a highly efficient, CO_2-specific enzyme catalyst, carbonic anhydrase (CA – E.C. 4.2.1.1). It has a turnover number of 1 million moles CO_2 per mole CA per second [10]. High permeability and selectivity are thus guaranteed.

The CA-involved reaction and the related mass transfer are complicated and a full understanding of CO_2 transport in such process is still not available. Schultz [11] analyzed the mass transfer of CO_2 across supported liquid membranes consisting of bicarbonate / carbonate / CA. The bicarbonate product inhibition of CA was treated akin to that of other monovalent anion inhibitors; K_{mi} was set at 1M. However, this model is insufficient for two reasons. First, the value of K_{mi} is much higher than the well-known value of K_m of HCO_3^-, which

is around 30 mM [12]. Second, he assumed a uniform transmembrane concentration of cationic species. In graphic representations derived from our simulations this is not the case (data not shown). Another difference is that they used a boundary layer approximation method to solve the model equations. This approach assumes chemical equilibrium in the liquid membrane except within regions close to the boundaries. At very low feed CO_2 concentration, this assumption will be invalid. In contrast, we used a rate-based analysis that allows dynamic evaluation of concentrations across the entire membrane thickness. This was achieved by numerical modeling of the CO_2 transfer across a liquid membrane facilitated by CA. The mechanism of CA-catalyzed CO_2 hydration / dehydration reactions was carefully examined. HCO_3^- inhibition of CA was treated as product inhibition, and was integrated into the transport equations. The resulting diffusion-reaction model was solved numerically across the whole liquid film using the finite difference method. We analyzed the effects of buffer concentration, CO_2 partial pressure and end product inhibition on CO_2 permeance. We then tested the validity of the model by a first order comparison between the numerically modeled data and the experimental results obtained under similar conditions.

Model

At steady state, conservation of each of the species in CLM is governed by following equation:

$$\frac{dN_i}{dx} = R_i \tag{1}$$

where x is the coordinate in the direction of transport, N_i the flux of species i, and R_i is the chemical reaction rate for species i.

From the Nernst-Planck equation,

$$N_i = [i]v - D_i\left(\frac{d[i]}{dx} + Z_i[i]\frac{F}{RT}\frac{dV}{dx}\right) \tag{2}$$

where v is the velocity, D_i the diffusivity if species i in the CLM, Z_i the charge of species i, F the Faraday's constant, R the ideal gas constant and V the diffusive potential. To simplify the solution, v and V are not considered in the calculations, as no convection exists and the effect of the electrical potential is very small [13].

The chemical reactions taking place in the CLM are:

$$\mathrm{Re}\,action\,1: \quad CO_2 + H_2O \Leftrightarrow H^+ + HCO_3^- \tag{3}$$

$$\mathrm{Re}\,action\,2: \quad CO_2 + OH^- \Leftrightarrow HCO_3^- \tag{4}$$

k_1 and k_{-1} are the forward and reverse reaction rate constant of reaction 1, respectively. k_2 and k_{-2} are the forward and reverse reaction rate constant of reaction 2. K_1 and K_2 are the chemical equilibrium constants for reactions 1 and 2, respectively.

The resulting CO_2 reaction rate expression is

$$R_{CO_2} = (k_1 + k_2[OH^-]) * [CO_2] - (k_{-1}[H^+] + k_{-2}) * [HCO_3^-] \quad (5)$$

The following two reactions (Reaction 3 and 4) are also involved in the CLM, but compared to the slow reactions 1 and 2, Reactions 3 and 4 are sufficiently rapid that chemical equilibrium may be assumed.

$$\text{Reaction } 3: \quad HCO_3^- \Leftrightarrow H^+ + CO_3^{-2} \quad (6)$$

$$\text{Reaction } 4: \quad H_2O \Leftrightarrow H^+ + OH^- \quad (7)$$

The chemical equilibrium constants are defined as

$$K_W = [H^+] * [OH^-] \quad (8)$$

$$K_3 = \frac{[H^+][CO_3^{-2}]}{[HCO_3^-]} \quad (9)$$

Applying electroneutrality to the CLM, we have

$$[H^+] + [M^+] = [OH^-] + [HCO_3^-] + 2 * [CO_3^{-2}] \quad (10)$$

Under the experimental conditions, $[H^+]$ and $[OH^-]$ are negligible compared to other ion concentrations (at pH = 8.0, $[H^+]$= 1E-8 M, and $[OH^-]$ =1E-6 M, $[HCO_3^-]$ and $[CO_3^{-2}]$ are larger than 1E-3 M). Therefore Equation 10 can be simplified to

$$[M^+] = [HCO_3^-] + 2 * [CO_3^{-2}] \quad (11)$$

From total carbon balance in the CLM, it follows that

$$N = N_{CO_2} + N_{HCO_3^-} + N_{CO_3^{-2}} = \Phi \quad (12)$$

where Φ is a constant.

Boundary conditions for the system are given in Equations 13-16.

$$N_{M^+} = 0 \quad (13)$$

With the assumption of negligible mass transfer resistance in the gas phase or the polymer separation membrane (i.e., when mass transfer resistance in the liquid is much greater), the flowing boundary conditions are assumed:

$$[CO_2] = HP_{CO_2,0} \quad x = 0 \quad (14)$$

and

$$[CO_2] = HP_{CO_2,L} \quad x = L \tag{15}$$

where P is the CO_2 partial pressure, H is Henry's constant and L is the CLM thickness.

When external mass transfer resistance is comparable to liquid mass transfer resistance, with steady state CO_2 transport through the CLM, we have

$$N = k_f([CO_2]_f - H[CO_2]_{f,x=0}) = k_s([CO_2]_s - H[CO_2]_{s,x=L}) \tag{16}$$

where k_f and k_s are the mass transfer coefficients at the feed and sweep sides, respectively. $[CO_2]_f$ and $[CO_2]_S$ are CO_2 concentrations in the bulk of the feed and sweep, respectively. $[CO_2]_{f,\ x=0}$ and $[CO_2]_{S,x=L}$ are the CO_2 concentrations at the feed side gas-liquid interface and sweep side gas-liquid interface.

Differentiating Equation 11 and combining with Equation 13, we have

$$\frac{d[HCO3^-]}{dx} = -2\frac{d[CO_3^{-2}]}{dx} \tag{17}$$

or

$$N_{CO_3^{-2}} = -\frac{1}{2}\frac{D_{CO_3^{-2}}}{D_{HCO_3^-}} N_{HCO_3^-} \tag{18}$$

For the boundary conditions shown in Equations 14 and 15, the problem can be easily solved. However, for boundary conditions with external mass transfer resistance, a trial and error method is needed to find the total CO_2 flux.

In this model, the un-catalyzed reaction of CO_2 and H_2O, the CA-catalyzed reaction of CO_2 and H_2O, and the CO_2 reaction with OH^- are considered as concomitant processes; all contribute to CO_2 transport. The CA-catalyzed reaction mechanism is derived from reversible enzymatic reactions.

The total CO_2 reaction rate is expressed as follows:

$$r_{CO_2} = \left(\frac{[E_0]k_{cat}}{([CO_2] + [HCO_3^-] * K_m^{CO_2} / K_m^{HCO_3^-} + K_m^{CO_2}} + k_{CO_2} + [OH^-] * k_{OH^-} \right) * ([CO_2] - [HCO_3^-]/K_{Eq}) \tag{19}$$

where k_{CO2} is the rate constant for the un-catalyzed CO_2 and H_2O reaction, k_{OH-} is rate constant for CO_2 and OH^- reaction. K_{Eq} is the chemical equilibrium constant for Reaction 1. Note that [OH-] is a very small number.

Let us define the following dimensionless variables and groups:

$\alpha=[CO_2]/[CO_2]_{x=0}$;

$$\beta=[HCO_3^-]/[M^+];$$
$$K_{11}=(L^2*kcat*[E]_0)/(D_{CO2}*[CO_2]_{x=0});$$
$$K_{22}=K_m^{CO2}*[M^+]\ (K_m^{HCO3-}*[CO_2]_{x=0});$$
$$K_{33}=K_m^{CO2}/[CO_2]_{x=0};$$
$$K_{44}=(L^2*kco_2)/D_{CO2};$$
$$K_{55}=(L^2*k_{OH-}*K_W)/(2*D_{CO2}*K_3);$$
$$K_{66}=-2*(L^2*[M^+]*kcat*[E]_0*K_3)/(D_{CO2}*[CO_2]_{x=0}\text{^}2*K_{Eq});$$
$$K_{77}=-2*(L^2*[M^+]*kco2*K_3)/(D_{CO2}*[CO_2]_{x=0}*K_{Eq});$$
$$K_{88}=-(L^2*[M^+]*K_W*k_{OH-})/(D_{CO2}*[CO_2]_{x=0}*K_{Eq});$$

where $[CO_2]_{x=0}$ is the concentration in equilibrium with the feed CO_2 concentration, .

The diffusion-reaction governing equation can be written as

$$\frac{d^2\alpha}{dy^2}=\frac{K_{11}\alpha}{\alpha+K_{22}\beta+K_{33}}+K_{44}\alpha+K_{55}*(\frac{\alpha}{\beta}-\alpha)+\frac{K_{66}\beta^2}{(\alpha+K_{22}\beta+K_{33})(1-\beta)}+\frac{K_{77}\beta^2}{1-\beta}+K_{88}\beta \quad (20)$$

Simulations were carried out by solving above 1-dimensional reactive transport equation given the stated boundary conditions. All physical properties such as gas solubilities and diffusivities were taken from available open literature sources. The finite difference method was adopted and the program implemented in Matlab®.

Experimental Method

Celgard X30-240 woven hollow fiber mats were arranged in an X-Y pattern with controlled mat layer spacing. Feed gas and argon sweep gas were delivered bore-side while the enzyme-salt mixture was delivered shell-side in the Z direction. An Environics mass flow controller controlled gas delivery. The dry gas streams were humidified via Nafion membrane hollow fiber arrays. Permeate and retentate gases were analyzed using an ABB Extrel residual gas mass spectrometer. The data were analyzed using Questor software for subsequent display. An illustration of the experimental apparatus is given in Figure 1.

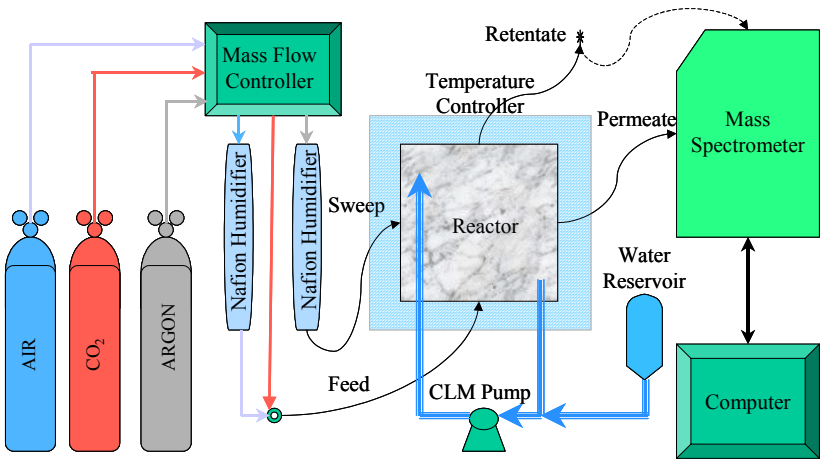

Figure 1. Schematic diagram of experimental apparatus

Results and Discussions

Simulations were performed using parameter sets from literature reports and the results compared to confirm the feasibility of our programs. Separation performance is highly dependent on both the process parameters and inherent reactor parameters, consequently simulations were carried out by varying numerous parameters such as enzyme concentration, liquid membrane composition and thickness, with the goal of maximizing the overall performance for a given CO_2 feed concentration.

Figure 2 shows a typical transmembrane concentration profile. Large CO_2 concentration gradients exist at two boundaries of the liquid membrane due to the CA-catalyzed facilitated transport chemical reactions. The choice of liquid membrane is critical to the CO_2 transport across the CLM. Facilitation of CO_2 transport comes from the bicarbonate and carbonate concentration gradients imposed onto the CO_2 concentration gradient. Higher bicarbonate / carbonate concentrations are needed for larger facilitation. However, higher salt concentration reduces the diffusivity and solubility of the gases and can inhibit the enzyme. Thus, there is a tradeoff of these factors to achieve the preferred choice of salt concentration to yield the best performance for a given concentration of CO_2 in the feed. As shown in Figure 3, for 1.0% CO_2 in the feed at 1 atm, the highest permeance occurs at a salt concentration of 0.5M. Of course, selectivity will increase with salt concentration.

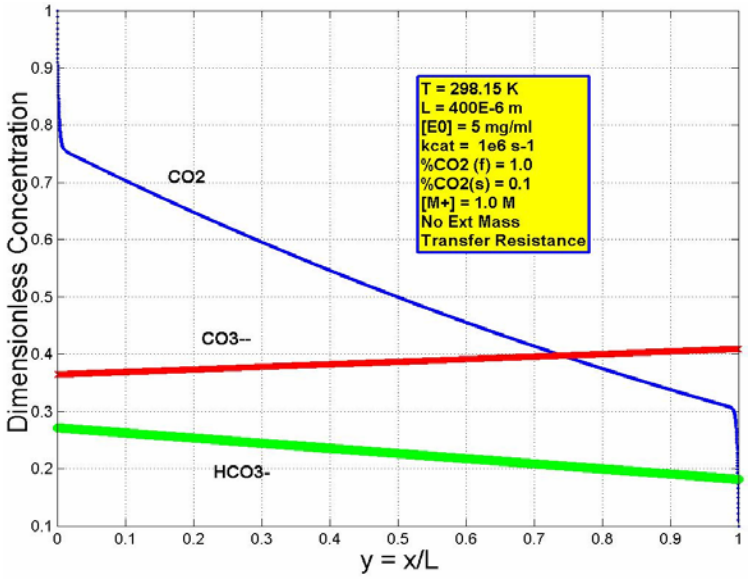

Figure 2. Transmembrane concentration profile

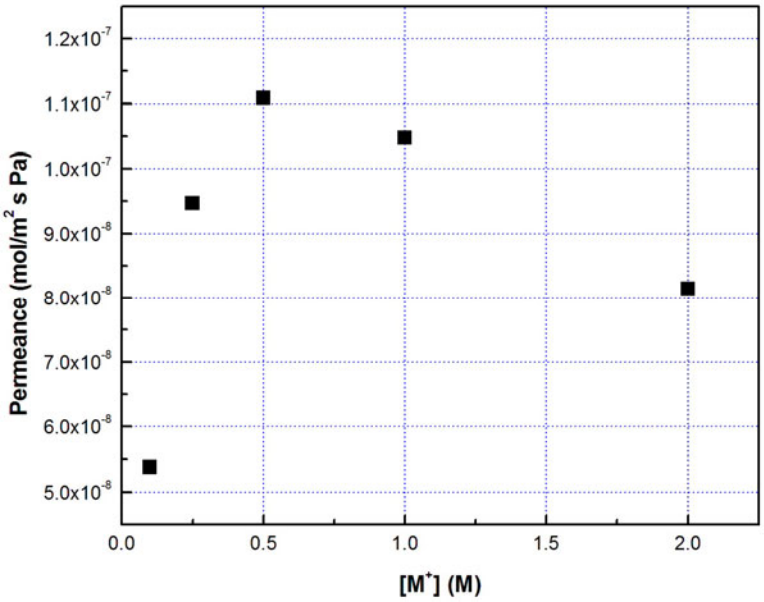

Figure 3. Effect of total metal concentration

Figure 4 illustrates the effect of liquid membrane thickness on the CO_2 permeance for the same set of parameters shown in Figure 2, for both CA-catalyzed and non-catalyzed CO_2 transport. As permeance is inversely proportional to liquid membrane thickness, thinner liquid membranes will give higher permeance. The key driver is lessened diffusion time. However, with thinner liquid membranes chemical reaction time will similarly reduced. As a result of these two factors, liquid membrane thickness exhibits a small effect on permeance. In contrast,

liquid membrane thickness plays a large role in selectivity and a thin liquid membrane will exhibit very poor selectivity.

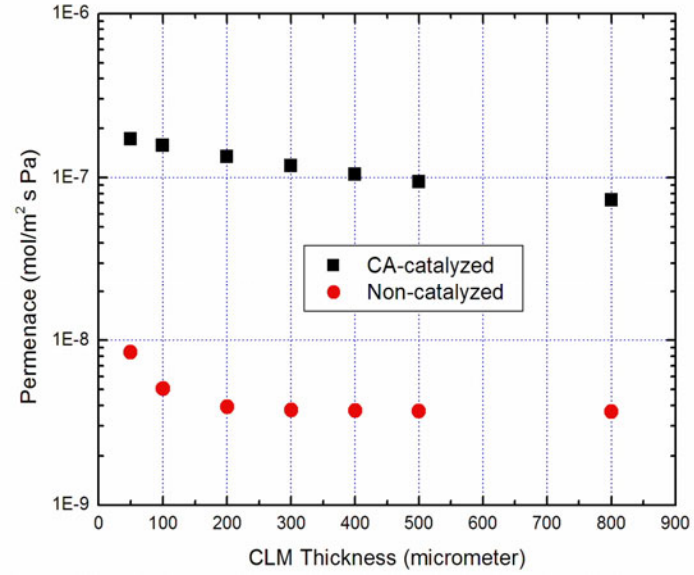

Figure 4. Effect of Liquid membrane thickness

The simulation results were compared with experimental data, as shown in Figure 5. Except at very low CO_2 concentration in the feed agreement between the model and experimental data is excellent. This difference is mostly like due to boundary layer mass transfer resistance.

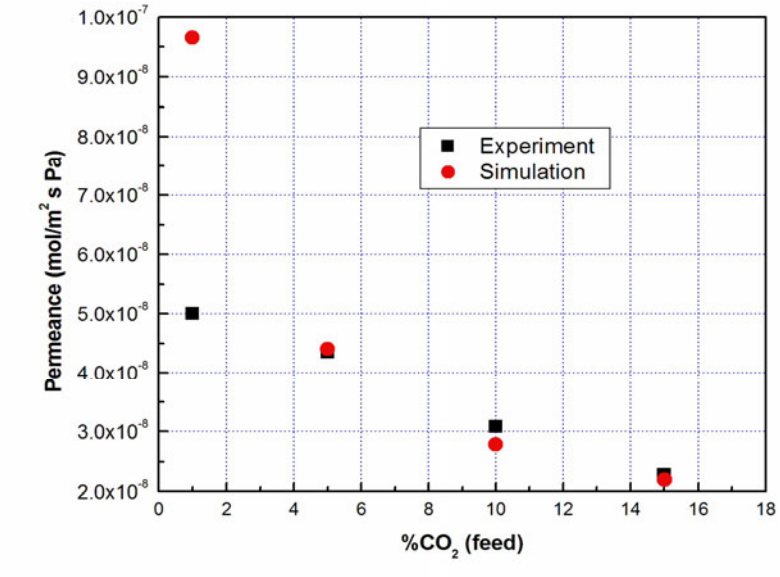

Figure 5. Comparison between simulation and experiment

Facilitated transport is limited by the chemical thermodynamics. The maximum facilitation occurs when all chemical reactions involved are at chemical equilibrium. In our simulations, we calculated the maximum CO_2 permeance for the following conditions: liquid membrane thickness = 400μm, Temperature = 298.15K, total pressure = 1atm and total salt concentration = 1M. The results are given in Table 1. As we can see, for 10% CO_2 concentration in the feed, the maximum permeance is 3.5E-8 mol/m^2 s Pa, and our measured CO_2 permeance is 3.35E-8 mol/m^2 s Pa, a value very close to the maximum possible. This proves the efficiency of CA.

Table 1. Maximum Facilitation at chemical equilibrium

CO_2%(Feed)	CO_2%(Sweep)	Facilitation factor	CO_2 permeance (mol/m^2 s Pa)
1.0	0.1	200	2.0E-7
5.0	0.5	64	6.3E-8
10.0	1.0	35	3.5E-8
20.0	2.0	18	1.8E-8
100.0	10.0	3.3	3.3E-9

We also tested the long-term stability of our system. The permeances of all gases are stable for over 6 days, the longest continuous period tested here (Figure 6). Previous studies of non-continuous test were continued for as long as 40 days. This indicates that CA maintained its activity (Maren assay tests of the liquid membrane confirmed this inference) and no significant membrane fouling was seen for the period of the test.

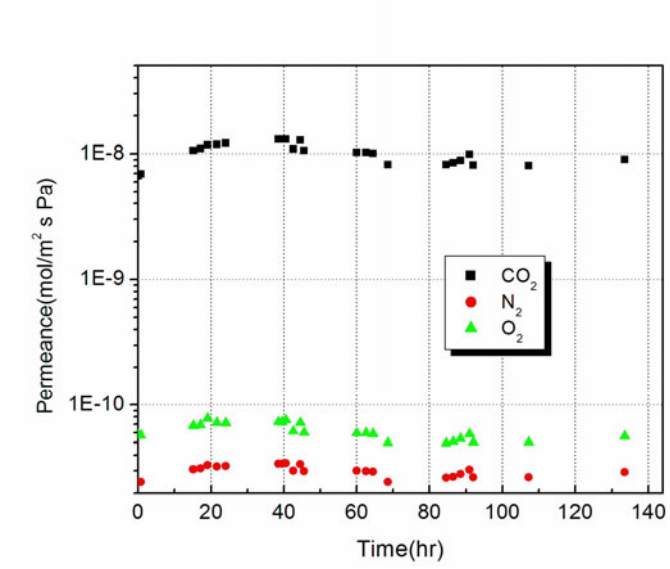

Figure 6. Long-time stability test of the system

Conclusions

We developed and solved numerically a mass transport model of CO_2 transfer through CA-catalyzed hollow fiber contained liquid membrane. The inhibition of HCO_3^- was carefully examined and implemented. Simulations examined the effect of CLM composition, membrane thickness, and other parameters. Simulated and experimental results are in excellent agreement.

The model will be a very useful tool for the selection of the preferred buffer solution and optimization of design of new reactors. This work has led to the development of new and improved approaches expected to yield better performance and greater efficiency.

Acknowledgements

We acknowledge support under grant DOE number DE-FG02-02ER83380 and NASA grant NAG9-1383.

References

[1] Kim, Y.-S., S.-M. Yang, "Absorption of carbon dioxide through hollow fiber membranes using various aqueous absorbents," *Sep. Purif. Technol.*, 21 (2000) 101-109.
[2] Feron, P. H. M., A. E. Jansen, "CO_2 separation with polyolefin membrane contactors and dedicated absorption liquids: performances and prospects," *Sep. Purif. Technol.*, 27 (2002) 231-242.
[3] Mavroudi M., S. P. Kaldis, G. P. Sakellaropoulos, "Reduction of CO_2 emissions by a membrane contacting process," *Fuel*, 82 (2003) 253-259.
[4] Cullinane J. T., G. T. Rochelle, "Carbon dioxide absorption with aqueous potassium carbonate promoted by piperazine," *Chem. Eng. Sci.*, 59 (2004) 3619-3630.
[5] Teromoto M. etc., "Separation and enrichment of carbon dioxide by capillary membrane module with permeation of carrier solution," *Sep. Purif. Technol.*, 30 (2003) 215-227.
[6] Gabelman, A., S.-T. Hwang, "Hollow fiber membrane contactors," *J. Mem. Sci.*,159 (1999) 61-106.
[7] Guha, A. K., S. Majumdar, K. K. Sirkar, "Facilitated transport of CO_2 through an immobilized liquid membrane of aqueous diethanolamine," *Ind. Eng. Chem. Res*, 29 (1990) 2093-2100.
[8] Trachtenberg, M. C., R. M. Cowan, S. L. Goldman, Y. Qin, E. Ford, "Carbon dioxide extraction from flue gas," *NAMS*, May 17-21, 2003, Jackson Hole, WY.
[9] Bao, L, D. A. Smith, S. L. Goldman, M. C. Trachtenberg, "Modeling CO_2 separation in a catalyzed liquid membrane," *NAMS,* June 26-30, 2004, Honolulu, Hawaii.
[10] Silverman D. N., "*Methods in Enzymol,"* 87 (1982) 732-752.
[11] Suchdeo S. R., J. S. Schultz, "Mass transfer of CO_2 across membranes: facilitation in the presence of bicarbonate ion and the enzyme carbonic anhydrase," *Biochim. Biophys. Acta*, 352 (1974) 412-440.
[12] Teaster T. B. etc., "Catalysis and inhibition of human carbonic anhydrase IV," *Biochemistry*, 36 (1997) 2669-2678.
[13] Jerry H. Meldon, Analysis of diffusion and reversible reaction in spatially confined systems, *Ind. Eng. Chem. Res*, 41 (2002) 456-463.